Mission REMOVEDD: REmoval of the Most OVErall Dangerous Debris

Joshua G. Holder
Senior, Rice University Mechanical Engineering, Houston TX, 77005

This paper outlines the REMOVEDD Mission, a mission which aims to rendezvous with, and then forcibly de-orbit, 20 of the most dangerous pieces of space debris as determined by the 2020 International Astronautical Congress. The mission involves 18 SmallSat size satellites equipped with commercially available Hall Effect Thrusters. First, each SmallSat will exploit J2 effects to match the Ω of each piece of debris. Next, a continuous thrust spiral trajectory is used to match the inclination and orbital radius of each piece of debris. Low-thrust phasing is performed via an adjustment of orbital altitude. Approximate solutions to the 3D orbital relative motion equations are used to design optimal fly-around and two-impulse docking maneuvers. Finally, both the SmallSat and space debris are de-orbited via slow spiral orbits to 400km in altitude. Mission trajectories are presented along with an analysis of the time taken, fuel spent, and estimated cost of this mission.

I. Nomenclature

Ω	=	right angle of the ascending node
e	=	orbit eccentricity
i	=	orbit inclination
a	=	semi-major axis
θ	=	true anomaly
θ_{circ}	=	angle of the spacecraft past the ascending node of a circular orbit

II. Introduction

As space activity continues to intensify, space debris has become an ever more critical issue – as of May 2021, 27,000 items in earth orbit are being tracked by the Department of Defense [1], not including countless more potentially dangerous objects which are too small to be effectively tracked. Left unchecked, the likelihood of a catastrophic collision potentially resulting in Kessler Syndrome [2] will continually increase.

Not all space debris is created equal, however. A paper presented at the 2020 International Astronautical Congress aimed to identify the top 50 "statistically most concerning" objects (SMCOs) in Earth orbit, using metrics like mass, encounter rates, and persistence. With so many pieces of debris in existence, any debris removal effort should prioritize highly dangerous objects on this list to have the greatest impact. Prominently featured on this list of SMCOs are 9000 kg Zenit-2 upper stages (coded SL-16 R/Bs by NORAD), used to launch Cold-War-era Soviet satellites and now orbiting Earth uncontrolled at 800km. The top 20 SMCOs are all SL-16 R/Bs, and conveniently, 18 of the 22 SL-16 R/Bs tracked by NORAD exist at inclinations of 71 degrees. This positions them particularly well for cheap removal en masse.

The mission will begin by launching a bus of 18 expendable SmallSats (SL-16s are too massive to be de-orbited with a satellite of CubeSat footprint) to an inclination of 71.0092 degrees. Upon reaching an orbit of the correct inclination, the SmallSats will be deployed from the satellite bus. At this point, each SmallSat must transfer to an orbit identical to the orbit of its target SL-16. First, the SmallSats utliize J2 effects to match the Ω, and perform continuous thrust spiral burns (as detailed in [3]) to match the a of each SL-16. The SmallSats will then conduct a low-thrust phasing maneuver to prepare for terminal rendezvous with the space debris. Once in position, each SmallSat will inspect the target with a fly-around maneuver and rendezvous with its target, attaching firmly with a robotic arm. Finally, while attached to the space debris, the SmallSat will again perform spiral burns over many orbits to lower the orbit radius to 350km, below important structures like the ISS and at an altitude at which drag from Earth's atmosphere will remove and de-orbit the object in just a few months.

Component	Estimated Mass (kg)
Satellite Body	40
Robotic Arm	15
Thrusters (RCS and Hall Effect)	5
Solar Panels	28.85
Propellant (Krypton)	205
Total	293.85

Table 1 SmallSat Estimated Mass Properties

III. Mission Details

A. SL-16 R/Bs Information

Each SL-16 has a dry mass of 9000 kg [4] with $a \approx 850km$, $i \approx 71°$. Notably, the e of each SL-16 is very near zero, with a maximum value of 0.0029 for SL-16 24298. This makes it reasonable to assume that the SL-16s are in circular orbits, which significantly simplifies many areas of the analysis. Additionally, the average SL-16 i is 71.0092 degrees; this will serve as the i at which the chaser satellites will begin the mission.

Given that the SL-16 orbits are assumed to be circular, each SL-16 θ must be converted to the equivalent θ_{circ}. This can be achieved by use of the following formula: $\theta_{circ} = \omega + \theta$, and following this, setting $\omega = 0$ as is the case for all circular orbits.

B. SmallSat Information

1. Satellite Propulsion

To minimize the cost of the mission, each chaser satellite must be as light and simple as possible. Because of the significant mass of the SL-16s (9000kg) and the large desired change in orbital altitude ($\sim$ 500km), the ΔV requirements of the mission are relatively high for a small satellite. This makes the mission a good candidate for electric propulsion methods, whose high ISPs will allow each satellite to carry a minimum amount of fuel.

The HT5k [5] is a standard commercially available Hall Effect Thruster which meets the specifications of the mission. This thruster can provide an ISP of 1600s at a thrust of 0.325N while receiving 5kW of power.

Each chaser satellite will also need to control its attitude in order to position its Hall Effect thruster for burns. To accomplish this, three standard RCS thrusters [6] will be used, along with a minimal amount of fuel.

2. Electrical Power

It is assumed that the satellite will require 6kW of power - 5kW for the Hall Effect Thruster and 1kW for miscellaneous other power requirements such as sensing, computing, thermal management, attitude control, and robotic arm control. Using industry standard SpectroLab solar panels [7], 6kW can be achieved with $16.39m^2$ of panel area, and accordingly $28.85kg$ of mass.

3. Latching Mechanism

It is necessary for each chaser satellite to have a mechanism to securely latch onto the SL-16s once in position. Significant development effort must be applied to this area, but in this analysis it is assumed that a robot arm is an appropriate solution for this aspect of the mission.

4. Mass Properties

Combining the aspects of the satellite mentioned above, Table 1 provides an estimate of the total mass properties of the SmallSats. Fuel is determined to be 200kg based on preliminary analysis performed on the mission profile. To validate this estimate of mass, note that Starlink Satellites are approximately 260kg [8].

e	Ω	i	ω	θ_{circ}	a
0	242.32 °	71.01 °	0 °	180 °	6887.1 km

Table 2 Optimized initial classical orbital elements of chaser satellites

C. Launch Vehicle Information

According to the Falcon 9 user guide [9], a Falcon 9 launch can deliver $8628kg$ of mass to an orbit of altitude $500km$ (calculated later in the paper) and $i = 71.0092°$. Assuming a bus of mass $1000kg$, the total weight of the payload required is $1000 + 18 * 288.85 = 6199.3kg < 8628kg$, and thus all 18 SL-16s can be de-orbited within a single launch of a Falcon 9.

IV. Mission Phases and Analysis

A. Initial Conditions

As mentioned above, the Falcon 9 launch vehicle will deposit all 18 SmallSats into a circular orbit at an altitude of 500km and an i of 71.0092°. This leaves the initial Ω and θ_{circ} to be defined, where θ_{circ} is an analog of true anomaly for circular orbits, defined as the angular distance past the ascending node.

Given a date and time of launch, Ω can be calculated by determining the arc length from the latitude of the launch site to the equator at an angle of 71.0092°. This mission launches on the descending section of the orbit, so the longitude of ascending node is equal to this arc length + 180°. Finally, Ω can be calculated by adding the longitude of the ascending node to the angle of the prime meridian at launch time + 8 minutes.

Given that a chaser satellite will need to match the Ω of each SL-16, it is desirable that the starting value of Ω is a minimum average distance to the Ω values of the SL-16s. An optimization is performed to select the minute on June 1st, 2022 at which launching results in the minimum average Ω difference between the initial chaser satellite position and the SL-16s. This results in a launch date and time of 23:14 PM Universal Time, June 1st, 2022. Accordingly, the set of classical orbital elements which describes the initial position of the chaser satellites is shown in Table 2.

B. Matching Ω, i, and Orbit Radius

While orbital altitude, i, and e are similar between all SL-16s, values of Ω are significantly dispersed, ranging from 9.1° to 308.1°. This means that even from an optimal starting orbit, some chaser satellites will have to change their Ω significantly. In [10], a method for achieving Ω change with low-thrust is presented, but it requires significant ΔV. Instead, J2 gravitational effects can be exploited to create a change in Ω. Here, it is assumed that the engineering model of J2 effects is sufficient. Using this formulation, the change in Ω can be calculated as:

$$\Delta\Omega = (\dot{\Omega}_{SL-16} - \dot{\Omega}_{chaser})\Delta t \tag{1}$$

where $\dot{\Omega}$ is calculated via equation 8.3 in [11].

After reaching the correct orbital plane, each chaser must change its i and a to match its associated SL-16. In Edelbaum's seminal paper [12], he outlines the low-thrust transfer between two inclined circular orbits as an optimal control problem. Since the time of its publication in 1961, several improvements have been published [13] [14]. These more recent studies attempt to increase the fidelity of the transfer by providing analytical solutions or accounting for a dynamic spacecraft mass, but for the purposes of this preliminary mission design and the small change in mass, Edelbaum's formulation is sufficient.

Here, there exists a tradeoff between ΔV and transfer time. As seen in Figure 1, as the starting orbital altitude approaches that of the target, ΔV required for the maneuver decreases linearly but transfer time increases exponentially. Based on this analysis, a starting orbital altitude of $500km$ was selected.

Using Edelbaum's method as detailed in [12], the time of the transfer and the associated $\Delta\Omega_{transfer}$ can be calculated. $\Delta\Omega_{init} = \Delta\Omega_{J2} + \Delta\Omega_{transfer}$ so $\Delta\Omega_{J2}$, the change caused by J2 effects, can be found. With this, the state vector of each chaser satellite can be specified from orbit insertion to the point at which a, i, and Ω are equal to that of its target SL-16.

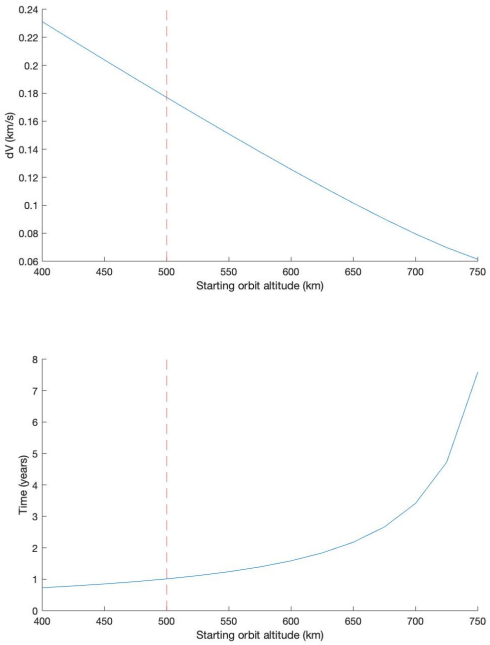

Fig. 1 Tradeoff between ΔV and Δt when varying starting orbit altitude

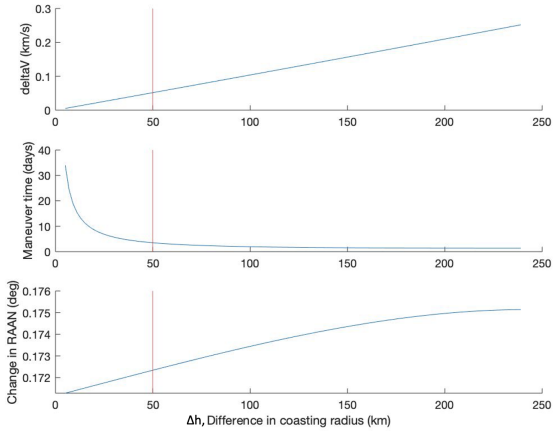

Fig. 2 Tradeoff between ΔV, Δt, and $\Delta\Omega$ when varying Δh in worst case transfer

C. Low-Thrust Phasing

At this point in the mission, $a_{SmallSat} = a_{SL-16}$, $i_{SmallSat} = i_{SL-16}$, $e_{SmallSat} = e_{SL16}$, $\Omega_{SmallSat} = \Omega_{SL-16}$, and $\omega_{SmallSat} = \omega_{SL-16}$, leaving only θ_{circ} to be matched prior to terminal rendezvous.

Many phasing maneuvers, including those mentioned in Chapter 7 of [11], rely on the assumption that burns are impulsive. Given that the chaser satellites in this mission utilize low-thrust Hall-Effect thrusters, this assumption does not hold. Instead, a low-thrust transfer as described in [15] and [16] must be performed. The basic principle for this transfer is as follows: If the chaser satellite needs to increase its θ_{circ} to reach the target satellite, it transfers into an orbit with some lower altitude h_{coast}, coasting at this new orbit's reduced period until the difference in θ_{circ} is made up. Finally, the chaser satellite transfers back into the initial orbit, now with a value of θ_{circ} matching that of the target (the reverse procedure is performed if the chaser satellite needs to decrease its initial θ_{circ}).

One complication arises in that while performing this transfer, the difference in radii between the chaser and the target orbit will induce an undesirable change in Ω which was just matched in the previous phase of the mission. A method to counteract this undesirable plane change is proposed in [15], but according to analysis, even in a worst case phasing maneuver, $\Delta\Omega \approx 0.172°$ and this effect can thus be neglected.

An appropriate value $\Delta h = |h_{target} - h_{coast}|$ must be selected to strike an appropriate balance between ΔV consumed and time taken to complete the phasing maneuver. As seen in Figure 2, as Δh increases, required ΔV and $\Delta\Omega$ increase but transfer time decreases. Based on this analysis, a value of $\Delta h = 50km$ was determined to yield a transfer acceptable in ΔV, Δt, and $\Delta\Omega$.

D. Terminal Rendezvous

The phasing maneuver performed in the previous section aims to deliver the chaser satellite at some $\Delta\theta_{circ}$ such that the chaser is an arc length of 60km away from the SL-16 on the orbit. This results in an initial relative position vector of:

$$\begin{bmatrix} asin(\Delta\theta_{circ}) & a - acos(\Delta\theta_{circ}) & 0 \end{bmatrix}$$

From this starting point, the chaser satellite will first travel to a relative position of $\begin{bmatrix} \pm 100m & 0 & 0 \end{bmatrix}$ in order to

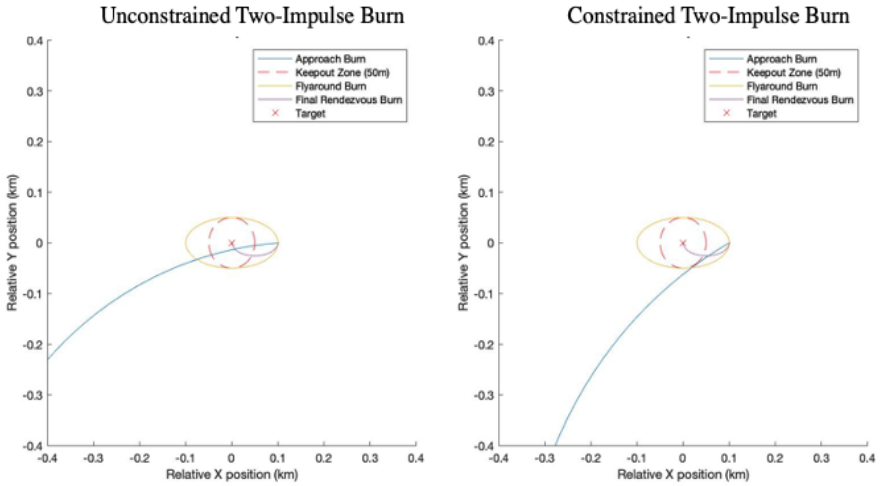

Fig. 3 Relative position over time for constrained and unconstrained two-impulse rendezvous and flyaround maneuvers

perform a fly-around maneuver for inspection. There is no clear analytical solution for the problem of low-thrust rendezvous, but several complex approaches have been developed which use optimal control theory [17] and, more recently, evolutionary algorithms [18] to find optimal solutions to the low-thrust rendezvous problem. However, after an initial analysis assuming optimal two-impulse burns, it was found that on average, the ΔV requirements were low enough that the Hall Effect thrusters could achieve the burns within $\sim$ 12% of the total transfer time, making an impulsive assumption reasonable in this case.

Therefore, both the approach and final rendezvous maneuvers are approximated as two-impulse rendezvous by using equation 7.48 in [11]. Similarly, the impulsive assumption allows a flyaround burn to be conducted according to equation 7.52 in [11].

To propagate the relative position of the chaser over the course of the burn, the solution to the first-order circular rendezvous equations are used, given that distances between the vehicles is small compared to the radius of earth, the orbits in question are circular, and there are no external accelerations over the course of the maneuver.

Rendezvous and fly-around maneuvers must be conducted during non-eclipse sections of the orbit. Given that the i of each chaser satellite is $\sim 71°$, the satellite is in an orbit with β significantly higher than $\beta_{crit} = sin^{-}1(\frac{1}{1+850/6371} = 61.92°$, the beta angle above which the satellite will never enter shade, for a significant portion of the year. Based on the dynamics of beta angle, this means that there are no constraints on the timing of the rendezvous and fly-around maneuvers other than for a few months in winter, and that lighting constraints can therefore be neglected in this analysis.

One complication that must be addressed in using an optimal two-impulse rendezvous is that it makes no consideration of the path of satellite between the starting and final locations. In many cases, an optimal burn will take the chaser satellite unacceptably near the target satellite during the approach burn. Because of this, the burn must be optimally designed to find the minimum ΔV burn which still satisfies a keep-out constraint. Figure 3 demonstrates this design consideration, as well as the the trajectories of the chaser satellite throughout the terminal rendezvous phase.

E. De-orbit

Once terminal rendezvous has been completed and the given chaser spacecraft is securely attached to its target SL-16, de-orbit can be initiated. Deorbit is defined as complete when the perigee altitude of the SmallSat-SL-16 system is <= $350km$, at which point the debris is below important LEO objects and will be de-orbited naturally within 3-20 days [11].

There are two possible methods to accomplish this: in Method 1, only perigee altitude is decreased by performing retro burns in the area around apogee during each orbit. In Method 2, continuous retro thrusting produces a spiral trajectory discussed above which reduces the radius of perigee and apogee simultaneously.

Given the non-impulsive nature of low-thrust maneuvers, analysis was conducted to determine the effects of gravity

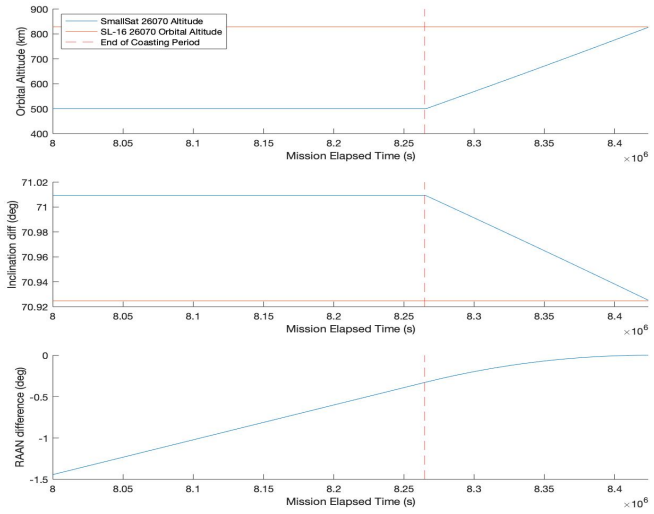

Fig. 4 Time history of chaser 26070 a, i, $\Delta\Omega$ over first phase of mission

loss on a de-orbit maneuver using Method 1. While Method 1 looked promising after preliminary analysis without gravity loss included, when taking these effects into account Method 2 vastly outperforms Method 1 in transfer time while consuming a similar amount of fuel, and was thus chosen for this mission.

V. Results

In this section, resulting standard trajectories for chaser satellites through the various phases of the mission will be presented, followed by an overall results section comprised of a detailed burn timeline, fuel usages by SmallSat, and other overall conclusions.

A. Sample Trajectory for Matching Ω, i, and Orbit Radius

Following the procedure outlined in Section IV.B, a software tool (matchOrbits.m) was developed which, given an initial set of classical orbital elements (circular orbits) for a chaser and target satellite and the mass of the spacecraft, will calculate a low-thrust transfer between the chaser and target orbit radii and inclinations, as well as the time to wait for the effects of J2 to affect Ω before starting the burn. The function will return the magnitude of the burn and transfer time, as well as a complete time history of orbital elements of the chaser and target satellite over the period of the transfer.

Figure 4 shows a sample trajectory for this phase of flight calculated with the described methodology. Note that $\Delta\Omega$ changes linearly until the transfer begins, at which point the rate of change approaches zero at the moment when $\Delta\Omega = 0$.

B. Sample Trajectories for Phasing

Following the procedure outlined in Section IV.C, a software tool (lowThrustPhase.m) was developed which, similar to matchOrbits.m, given an initial set of classical orbital elements (circular orbits) for a chaser and target satellite, a desired Δh (as defined in Section IV.C), and the mass of the spacecraft, will calculate a low-thrust phasing maneuver to deliver the chaser spacecraft an arc length of 60km away from the target satellite in preparation for terminal rendezvous. The function will return the magnitude of the burn and transfer time, as well as the misalignment in Ω created by the maneuver and a complete time history of orbital elements of the chaser and target satellite over the period of the transfer. This software is provided to MECH 578 students in a *pro bono* capacity.

Figure 5 demonstrates the trajectories generated by this function, which has the capability to determine whether a speedup or slowdown is appropriate to phase in the minimum amount of time. SL-16 17974 starts 20° ahead of chaser 17974 in orbit, and accordingly the tool determines that the chaser should decrease orbital radius, coast briefly, and transfer back to the initial orbit. Conversely, SL-16 22285 is 170° behind its respective chaser at the start of the

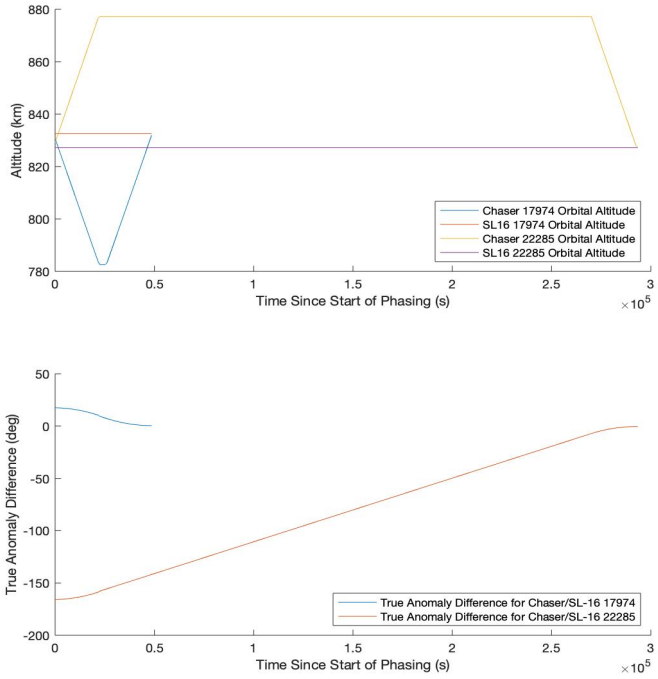

Fig. 5 Time history of chaser 17974 and 22285 a, θ_{circ} over the phasing maneuver

maneuver, and thus the chaser increases its orbital altitude and coasts for a significantly longer amount of time before returning to the original orbit.

C. Sample Trajectories for De-orbit

Following the procedure outlined in Section IV.E, a software tool (deorbit.m) was developed which, given an initial set of classical orbital elements (circular orbit) for a spacecraft a desired de-orbit radius (350km in the case of the REMOVEDD mission), and the mass of the spacecraft, will calculate a low-thrust de-orbit maneuver to deliver the chaser spacecraft to a circular orbit with the desired radius. The function will return the magnitude of the burn and transfer time, as well as a complete time history of orbital elements of the spacecraft over the period of the de-orbit.

D. Mission Sensitivities

The mission is robust to changes in several parameters. An error in launch time or parameters is not a significant issue: because of the lack of precise timing windows, such an error would simply potentially increase the time needed to correct Ω errors with J2, or increase the fuel needed to change inclinations. Once in orbit, the continuous nature of most of the burns means that a slight timing error is not likely to have a significant impact on the trajectory of the satellite.

Finally, changing the thrust of the motor has a significant impact on the mission, but does not make the mission infeasible. For example, if the thrust of the motor is lowered to 0.1N, the average time to deorbit a SL-16 increases $\sim$ 200 days to 681.5732 days, largely due to the increase in time taken to de-orbit.

E. Overall Mission Trajectories

Tables 3 and 4 provide a information needed to obtain the full time history of motion for each of the 18 SmallSats involved in the mission, excluding detailed information on terminal rendezvous, which is outside the scope of this project.

Figure 6 provides a breakdown of the fuel used in each phase of flight. Notably, the de-orbit phase consumes the vast majority of the fuel because of the greatly increased mass of the combined spacecraft during this phase of flight.

SmallSat ID	**Time of Start of Burn to Match a and i (days)**	**Magnitude of Burn ΔV (km/s)**	**Time of Start of De-orbit burn (days)**	**Magnitude of De-orbit Burn ΔV (km/s)**	**Time of Full De-orbit (days)**
Comments	-	Continuous burn, always in the direction of velocity vector	-	Continuous burn, always opposite the direction of velocity vector	-
16182	208.4240	0.1824	214.2061	0.2647	301.7751
17590	535.3002	0.1783	540.1742	0.2615	626.6704
17974	397.4522	0.1830	400.2646	0.2615	486.7772
19120	616.4253	0.1793	619.9388	0.2634	707.0755
19650	140.6278	0.1756	143.8653	0.2598	229.8008
20625	104.3058	0.1925	108.2379	0.2701	197.5733
22220	121.9559	0.1759	126.0066	0.2601	212.0308
22285	325.7656	0.1804	331.3717	0.2588	416.9722
22566	953.0995	0.1904	957.6475	0.2712	1047.3
22803	141.4500	0.1852	145.8428	0.2694	234.9713
23088	911.6502	0.1770	917.2588	0.2538	1001.2
23405	472.9812	0.1794	477.3838	0.2597	563.3015
23075	366.7552	0.1766	369.3664	0.2533	453.1662
24298	185.0723	0.1831	190.7357	0.2664	278.8545
25407	863.2212	0.1786	866.2294	0.2560	950.9096
26070	95.6678	0.1761	98.2732	0.2595	184.1056
28353	595.0466	0.1789	600.7146	0.2630	687.7239
31793	49.0072	0.1732	54.2565	0.2541	138.2994

Table 3 Timing and magnitude information on initial and de-orbit burns for all 18 SmallSats

Figure 7 provides a breakdown of the time spent in each phase of flight. By this metric, the time spent waiting to match Ω using J2 effects is, for most satellites, the major contributor to the length of flight.

Radiation is a significant concern with such a long mission timeline (although below the Van Allen belt), with a maximum exposure of 31150 rads. Additionally, the risk of other impacts with other debris or satellites while deorbiting the SL-16 may be a significant concern and must be addressed in future design, but is outside the scope of this study.

VI. Conclusion

This paper outlines the design of Mission REMOVEDD, which aims to de-orbit the top 20 most dangerous space debris objects currently being tracked in LEO using SmallSats outfitted with commercially available Hall Effect Thrusters. Based on analysis, it is clear that this mission is feasible, achieving de-orbit for all twenty SL-16s in an average of 484.24 days and a maximum of 1047 days.

Furthermore, such a mission would be relatively affordable: the mission objectives were achieved in just one Falcon 9 launch, and with satellites relying heavily on off-the-shelf hardware. Higher-fidelity development and analysis should focus on the mechanism of autonomously docking to uncooperative space debris, but as a proof of concept Mission REMOVEDD is a success.

Acknowledgments

The author would like to thank Dr. P. Rodi for his guidance throughout the process.

SmallSat ID	**Time of Start of Phasing (days), Increase/Decrease of Radius**	**Length of Coasting Period (days)**	**Length of Phasing Maneuver (days)**	**Magnitude of Phasing Burns ΔV (km/s)**
Comments	Increase = burn in the direction of velocity Decrease = burn in the opposite direction of velocity	-	-	Continuous burn, direction defined in other comment
16182	210.3323, decrease	3.0304	3.5633	0.0517
17590	537.1656, decrease	2.1650	2.6987	0.0517
17974	399.3677, decrease	0.0530	0.5866	0.0211
19120	618.3014, increase	0.8027	1.3305	0.0512
19650	142.4651, increase	0.5646	1.0933	0.0512
20625	106.3197, decrease	1.0770	1.6083	0.0515
22220	123.7970, increase	1.3740	1.9027	0.0512
22285	327.6535, increase	2.8815	3.4103	0.0512
22566	955.0917, decrease	1.7154	2.2465	0.0515
22803	143.3884, decrease	1.6133	2.1451	0.0516
23088	913.5026, decrease	2.9137	3.4492	0.0519
23405	474.8581, decrease	1.6812	2.2153	0.0518
23075	368.6031, decrease	0	0.4559	0.0128
24298	186.9883, decrease	2.9138	3.4408	0.0516
25407	865.0902, decrease	0.3010	0.8304	0.0513
26070	97.5108, increase	0	0.4558	0.0512
28353	596.9192, decrease	2.9515	3.4848	0.0517
31793	50.8194, decrease	2.5944	3.1299	0.0519

Table 4 Timing and magnitude information on phasing burns for all 18 SmallSats

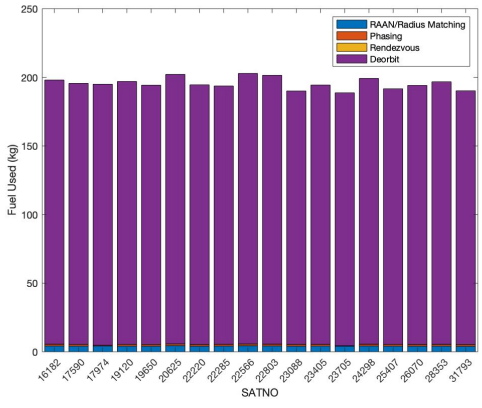

Fig. 6 Time spent in each phase of flight for all 18 SmallSats

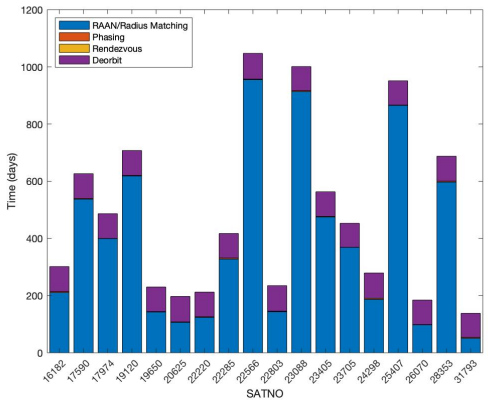

Fig. 7 Fuel usage by phase of flight for all 18 SmallSats

References

[1] Garcia, Mark. "Space Debris and Human Spacecraft." NASA, NASA, 14 Apr. 2015, https://www.nasa.gov/mission$_pages/station/news$

[2] Kessler, D. J., and Cour-Palais, B. G. (1978), Collision frequency of artificial satellites: The creation of a debris belt, J. Geophys. Res., 83(A6), 2637– 2646, doi:10.1029/JA083iA06p02637.

[3] Edelbaum, T N. Propulsion Requirements for Controllable Satellites. ARS(Am. Rocket Soc.) J.: N. p., 1961. Web. doi:10.2514/8.5723.

[4] "Orbital Debris Quarterly News.", Volume 15, Issue 2. orbitaldebris.jsc.nasa.gov, https://orbitaldebris.jsc.nasa.gov/quarterly-news/pdfs/odqnv15i2.pdf.

[5] Ducci, Cosimo. "Development and Performance Characterization of a 5 KW Class Hall-Effect Thruster." Internation Electric Propulsion Conference, 6 July 2015.

[6] Hydrazine Thrusters Specifications. Ariane Group, http://www.space-propulsion.com/brochures/hydrazine-thrusters/hydrazine-thrusters.pdf.

[7] "PV Solar Panel Specifications." Spectrolab.com, Spectrolab, https://www.spectrolab.com/DataSheets/Panel/panels.pdf.

[8] "NASA - NSSDCA - Starlink Details." NASA Space Science Data Coordinated Archive, NASA, https://nssdc.gsfc.nasa.gov/nmc/spacecra 045Camp;lang=en.

[9] "Falcon 9 User Guide", SpaceX

[10] Pollard, James. "Evaluation of Low-Thrust Orbital Maneuvers." 34th AIAA/ASME/SAE/ASEE Joint Propulsion Conference and Exhibit, 1998, https://doi.org/10.2514/6.1998-3486.

[11] Chobotov, Vladimir A. Orbital Mechanics. American Institute of Aeronautics and Astronautics, 2002.

[12] Edelbaum, Theodore N. "Propulsion Requirements for Controllable Satellites." ARS Journal, vol. 31, no. 8, 1961, pp. 1079–1089., https://doi.org/10.2514/8.5723.

[13] Casalino, Lorenzo, and Guido Colasurdo. "Improved Edelbaum's Approach to Optimize Low Earth/Geostationary Orbits Low-Thrust Transfers." Journal of Guidance, Control, and Dynamics, vol. 30, no. 5, 2007, pp. 1504–1511., https://doi.org/10.2514/1.28694.

[14] Di Carlo, Marilena, and Massimiliano Vasile. "Analytical Solutions for Low-Thrust Orbit Transfers." Celestial Mechanics and Dynamical Astronomy, vol. 133, no. 7, 2021, https://doi.org/10.1007/s10569-021-10033-9.

[15] Pollard, James. "Low-Thrust Maneuvers for Leo and Meo Missions." 35th Joint Propulsion Conference and Exhibit, 1999, https://doi.org/10.2514/6.1999-2870.

[16] Shang, Haibin, et al. "Design and Optimization of Low-Thrust Orbital Phasing Maneuver." Aerospace Science and Technology, vol. 42, 2015, pp. 365–375., https://doi.org/10.1016/j.ast.2015.02.003.

[17] Kechichian, Jean Albert. "Optimal Low-Thrust Rendezvous Using Equinoctial Orbit Elements." Acta Astronautica, vol. 38, no. 1, 1996, pp. 1–14., https://doi.org/10.1016/0094-5765(95)00121-2.

[18] Wall, Bradley J., and Bruce A. Conway. "Shape-Based Approach to Low-Thrust Rendezvous Trajectory Design." Journal of Guidance, Control, and Dynamics, vol. 32, no. 1, 2009, pp. 95–101., https://doi.org/10.2514/1.36848.